

Geophysical fingerprint of the 4-11 July 2024 eruptive activity at Stromboli volcano, Italy.

Luciano Zuccarello^{1,2}, Duccio Gheri¹, Silvio De Angelis^{2,1}, Riccardo Civico³, Tullio Ricci³, Piergiorgio Scarlato³.

¹Istituto Nazionale di Geofisica e Vulcanologia, Sezione di Pisa, via Cesare Battisti, 53, 56125, Pisa, Italy.

²School of Environmental Sciences, University of Liverpool, 4 Brownlow Street, L69 3GP, Liverpool, UK.

³Istituto Nazionale di Geofisica e Vulcanologia, Sezione di Roma 1, via di Vigna Murata, 605, 00143, Roma, Italy.

Correspondence to: Luciano Zuccarello (luciano.zuccarello@ingv.it); Duccio Gheri (duccio.gheri@ingv.it)

Codice campo modificato

Abstract. Paroxysmal eruptions, characterized by sudden and vigorous explosive activity, are frequent common events at many open-vent volcanoes. Stromboli volcano, Italy, is well-known for its nearly continuous degassing activity and mild explosions from the summit craters, occasionally punctuated by energetic, short-lived paroxysms. Here, we analyse multi-parameter geophysical data recorded at Stromboli in early July 2024, during a period of activity that led to a paroxysmal eruption on 11 July. We use seismic, infrasound and ground deformation data, complemented by visual and Unoccupied Aircraft System observations, to identify key geophysical precursors to the explosive activity and to reconstruct the sequence of events. Elevated levels of volcanic tremor and Very Long Period (VLP) seismicity accompanied moderate explosive activity, lava emission and small collapses from the North crater, leading to a major explosion on 4 July 2024 at 12:16 (UTC). Collapse activity from the North crater area continued throughout July 7, while effusive activity occurred from two closely-spaced vents located within the Sciara del Fuoco slope, on the Northwest flank of the volcano. On 11 July, a rapid increase in ground deformation preceded, by approximately 10 minutes, a paroxysmal event at 12:08 (UTC); the explosion produced a 5 km-high eruptive column and pyroclastic density currents along Sciara del Fuoco. Our observations suggest that the early activity in July was linked to eruption of resident magma within the shallowest parts of the volcano plumbing. This was followed by lowering of the magma level within the conduit system as confirmed by the location of newly opened effusive vents. The rapid inflation observed before the paroxysmal explosion on 11 July is consistent with the rapid expansion of gas-rich magma rising from depth, as frequently suggested at Stromboli during energetic explosive events. Rapid ground deformation before the paroxysmal explosion on July 11 is consistent with the expansion of a gas-rich magma rising from depth, similar to past energetic explosive events at Stromboli. Our results provide additional valuable insights into the eruptive dynamics of Stromboli and other open-conduit volcanoes, and emphasize the importance of integrated geophysical observations for understanding eruption dynamics, their forecasting and associated risk mitigation. Our findings offer valuable insights into Stromboli's eruptive dynamics and other open-conduit volcanoes, highlighting the importance of integrated geophysical observations for understanding eruption dynamics, forecasting, and associated risk mitigation.

Commentato [I1]: Unify upper or lower case for the crater's name

Commentato [I2]: Delete “,”

1 Introduction

Stromboli is an open conduit stratovolcano located in the Tyrrhenian Sea, off the northern coast of Sicily; its activity is characterized by continuous degassing and frequent, small-to-moderate, explosions occurring every few minutes from the summit craters, the well-known Strombolian activity. However, activity at Stromboli can rapidly escalate into more energetic events, referred to as major explosions, which eject centimeter-to-meter-sized ballistic projectiles; at times, sustained explosive activity is accompanied by partial collapses of the crater rim ~~due to the instability of accumulated material, and increased magmatic pressure within the conduit system~~ (Gurioli et al., 2013; Di Traglia et al., 2024). Since 2019, major explosions at Stromboli have occurred with a frequency of about 4-5 events per year ejecting pyroclastic material to heights over a hundred meters, which can travel beyond the summit crater area and potentially affect tourist paths (Rosi et al., 2013; Gurioli et al., 2013). ~~During periods of~~ heightened ~~states of~~ activity, Stromboli may also experience paroxysms, that is highly energetic eruptions that generate eruptive columns exceeding 4 km in height, ballistics of up to 2 m in diameter and significant collapse activity from the summit crater areas (Fig. 1). Paroxysms can be accompanied by the emplacement of pyroclastic density currents (PDCs) along the Sciara del Fuoco (SdF, Fig. 1a), which can enter the sea and travel up to 2 km from the shoreline with demonstrated potential to trigger tsunamis (Rosi et al., 2006; Calvari et al., 2006; D'Auria et al., 2006; Ripepe and Lacanna, 2024). Although paroxysms are less frequent than major explosions, with an average occurrence of just one every four years since 2003, they are the most impactful hazard for the island of Stromboli (Rosi et al., 2013). ~~For instance, A the~~ recent paroxysm ~~occurred~~ on 3 July, 2019, resulted in a fatality (Giudicepietro et al., 2020; Giordano and De Astis, 2020; Andronico et al., 2021).

Unrest and eruption at Stromboli generate a broad range of geophysical signals. Nucleation and coalescence of gas bubbles into gas slugs (Sparks, 2003; Burton et al., 2007; Caricchi et al., 2024), and their ascent within the conduit generates characteristic seismic and deformation signals (Marchetti et al., 2009); gas slug bursting at the top of the magma column produces infrasound waves (Colò et al., 2010). Real-time detection and monitoring of these signals are crucial for risk mitigation at Stromboli ~~as~~, in the recent past, major explosions and paroxysms have ~~frequently~~ been anticipated by detectable changes in geophysical signals between tens of seconds and minutes before their occurrence (Giudicepietro et al., 2020; Ripepe et al., 2021a; Longo et al., 2024).

Except for the 2019 eruptive activity, the most intense in recent years, Stromboli's paroxysms are typically preceded by periods of lava effusion, or a general increase in surface activity that lasts for several days (Ripepe et al., 2009; Valade et al., 2016). Several studies have suggested that effusive eruptions may act as a trigger for paroxysmal explosions through a mechanism of decompression of the volcano plumbing system, evidenced by a drop in magma levels within the conduit (Aiuppa et al., 2010; Calvari et al., 2011; Ripepe et al., 2017). The most significant effusive event in terms of its volume occurred between December 2002 and July 2003 (Ripepe et al., 2017), which caused landslides, triggered a partial collapse of the SdF and culminated in a paroxysm on 5 April, 2003; this was the first large-scale paroxysmal event ~~on~~ recorded since 1985 (Calvari and Nunnari, 2023). However, it should also be noted that effusive eruptions are not necessarily followed by paroxysms. An example is the

65 November 2014 effusive eruption, which did not lead to paroxysmal activity (Rizzo et al., 2015). At the other end of the
 66 spectrum lies the paroxysm of July 2019, for which no clear increase in activity prior to the main event was recorded. As
 67 highlighted by Laiolo et al. (2022), thermal and gas flow levels had slightly increased but remained below "alert" thresholds.
 68 Multi-parameter data are crucial to understand unrest at Stromboli and to detect transitions between low-to-moderate activity
 69 and more explosive phases (Pistolesi et al., 2011; Andronico et al., 2021). A variety of –Several– models account for the
 70 occurrence and characteristics of explain the ordinary seismic activity signal recorded at Stromboli and similar volcanoes (e.g.,
 71 Chouet et al., 2008; Suckale et al., 2016; Ripepe et al., 2021b). Petrological analyses suggest Stromboli’s conduit is stratified,
 72 with two types of magma: highly porphyritic (HP) and low-porphyritic (LP) (Bertagnini et al., 2003; Francalanci et al., 2004,
 73 2005). Eruptions are believed to result from gas slugs rising through the HP magma, which acts as a viscous plug controlling
 74 their ascent and explosion (Sparks, 2003; Burton et al., 2007; Aiuppa et al., 2010; Caricchi et al., 2024). A recent model by
 75 Caricchi et al. (2024) suggests that instability of gas-rich foam layers at the base of magma column could also trigger
 76 paroxysmal explosions. Several conceptual models have been proposed accounting for the ordinary seismic activity observed
 77 at Stromboli and other similar volcanoes (e.g., Chouet et al., 2008; Suckale et al., 2016; Ripepe et al., 2021b). Petrological
 78 analyses of erupted products suggest the presence of a stratified conduit at Stromboli, consisting of two types of magma
 79 (Bertagnini et al., 2003; Francalanci et al., 2004; Francalanci et al., 2005). The upper conduit is thought to host highly
 80 porphyritic (HP) magma that is water-poor and rich in phenocrysts, and is erupted as scoria during ordinary activity; on the
 81 other hand, magma in the lower conduit is gas-rich, low-porphyritic (LP), and typically erupted as pumice alongside HP scoria
 82 and lithic blocks removed from conduit walls. Eruptive activity at Stromboli is inferred to be controlled by the buoyant ascent
 83 and bursting of gas slugs (Sparks, 2003; Burton et al., 2007; Caricchi et al., 2024; Aiuppa et al., 2010) from the top of the LP
 84 magma, rising through the more crystalline HP magma acting like a viscous fluid or a rigid plug and controlling the final ascent
 85 and explosion of the slugs (Suckale et al., 2016). A recent model (Caricchi et al., 2024) shows that the instability of gas-rich
 86 and low-density foam layers at the base of the magma column could also potentially trigger paroxysmal explosions at open
 87 conduit volcanoes.
 88 In this study, we report on the most recent paroxysm at Stromboli, which occurred on 11 July 2024, following after a month
 89 of unrest at the summit craters, as reported by the Istituto Nazionale di Geofisica e Vulcanologia (INGV) (INGV-OE, 2024).
 90 We analyse the precursory geophysical activity leading up to the paroxysm based on seismic, infrasound and ground
 91 deformation data gathered by the INGV monitoring network, complemented by observations conducted with an-Unoccupied
 92 Aircraft Systems (UAS) during the study period. The UAS imagery provides a valuable tool to interpret geophysical data and
 93 understand the conditions leading up to the paroxysm on 11 July, offering a high-resolution reconstruction of the eruptive
 94 events and associated morphological changes at the volcano. Unless, otherwise stated, all descriptions of surface activity in
 95 this manuscript are from direct field observations by the authors during the study period.

Commentato [I3]: FROM REV3: 1. However, I found some parts in the introduction to be too extensive. It might be better to move the part of the conceptual models and other geological studies (line 65-76) into the discussion section instead, since the mentioned studies already focus on discussing the possible mechanisms generating paroxysmal eruptions in Stromboli.

Commentato [I4]: Delete “by”

Commentato [I5]: Delete “,”

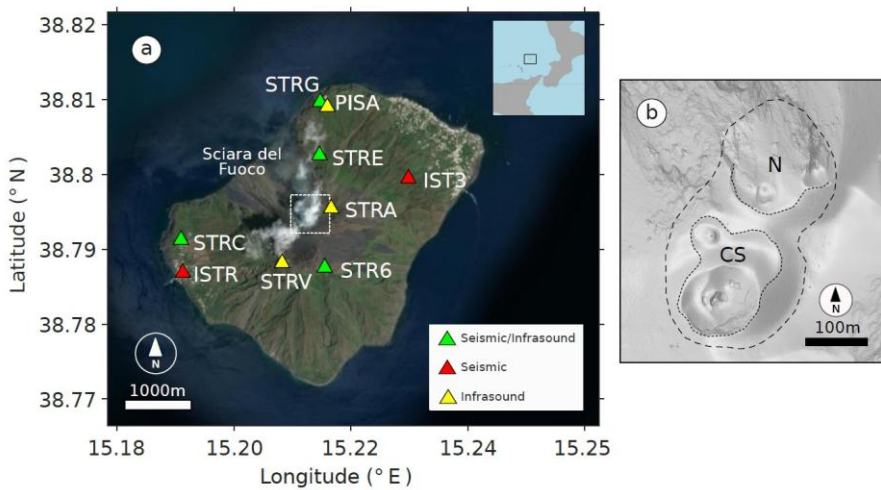


Figure 1: a) Map of monitoring network at Stromboli, showing the locations of seismo-acoustic, seismic, and infrasound sensors. The inset shows the location of Stromboli volcano in Italy (MATLAB Mapping Toolbox). b) Detail of the summit area of Stromboli, corresponding to the white dash-line square in a), showing the North (N) and Center-South (CS) summit crater areas.

2 Chronology of eruptive activity during 3-11, July, 2024

The activity bulletins issued by INGV (see Data Availability), from 24 May until the early days of July, reported an increase in surface activity at Stromboli, particularly from the North (N) crater area (Fig. 1b), characterized by continuous and intense spattering, that is quasi-continuous emission of pyroclastic material through sequential, small-to-moderate, explosions ejecting ballistics at heights of ~10-20 m above the vent (Harris and Ripepe, 2007; Giudicedipietro et al., 2021) (Fig. 2a). The average frequency of explosions fluctuated between 13 (medium) and 16 (high) events/hour with spattering occasionally leading to lava flows along the SdF (Fig. 1a). On 23 and 28 June, lava flows began, following intense spattering from the N crater, converging into a canyon-like structure created by previous PDC activity in October 2022 (Di Traglia et al., 2024). Sulfur dioxide (SO₂) and carbon dioxide (CO₂) emissions remained at average levels, as did the carbon-to-sulfur (C/S) ratio (INGV-OE, 2024).

On 3 July, at 16:35 UTC, intense spattering was observed from a vent located within the N crater sector, leading to a sequence of partial collapses of the N crater rim, which also remobilized material that had been erupted in the preceding days. These collapses mostly consisted of cold material with a minor contribution of hot deposits. At 17:02 UTC, a lava flow began from the same vent, accompanied by spattering and moderate explosions (Fig. 2b). The activity continued throughout the night, with lava fronts moving down to an elevation of 550-600 m a.s.l..

ha formattato: Colore carattere: Rosso

ha formattato: Non Evidenziato

ha formattato: Colore carattere: Rosso

Commentato [16]: The eruptive chronology from July 3 to 11, begins by describing the activity from May 24. Perhaps the authors could change the title of this section

ha formattato: Colore carattere: Rosso, Non Evidenziato

ha formattato: Colore carattere: Rosso

Commentato [17]: Unify the date typescript format along the text: e.g. 24 May or May 24

ha formattato: Colore carattere: Rosso

ha formattato: Pedice

ha formattato: Pedice

On 4 July, at 12:46-11 UTC, a major explosion occurred from the N crater and, at 14:10 UTC, a new lava flow emerged at the base of the N crater area at ~700 m a.s.l., advancing towards Bastimento and Filo di Fuoco, located along the northeast boundary of SdF. After about one hour, a second lava flow started at an elevation of ~580 m a.s.l., which reached the sea. At 16:15 UTC, another vent opened at ~510 m a.s.l., producing a third lava flow accompanied by PDCs that rapidly descended the SdF into the sea (Fig. 2c). During the evening of 4 July, and throughout the following night, lava flow activity continued, accompanied by occasional collapses of pyroclastic materials.

Between 5-6 July, 83 landslide events were observed, while effusive activity fluctuated and lava emission moved further downslope originating from two new eruptive vents at ~485 m a.s.l. (Fig. 2d). The flow formed a delta at the shoreline and steam plumes were observed caused by magma-seawater interaction. Explosive activity from the summit craters halted at the beginning of the effusive phase.

On 11 July, at 12:08 UTC, a paroxysmal eruption occurred from the N crater area, producing an ash plume ~5 km high, which dispersed towards the southwest (Fig. 2e). Shortly after, a pyroclastic flow rapidly advanced along the SdF, which triggered a small-scale tsunami wave. The paroxysmal phase ended with a series of secondary and less intense PDCs.

In the following hours, effusive activity ceased, and no further explosions were observed, except for a minor event on 12 July, at 08:28 UTC (Fig. 2a), which was followed by a small collapse event in the N crater area.

ha formattato: Colore carattere: Rosso

Commentato [18]: please clarify meaning or delete
 ha formattato: Colore carattere: Rosso, Barrato

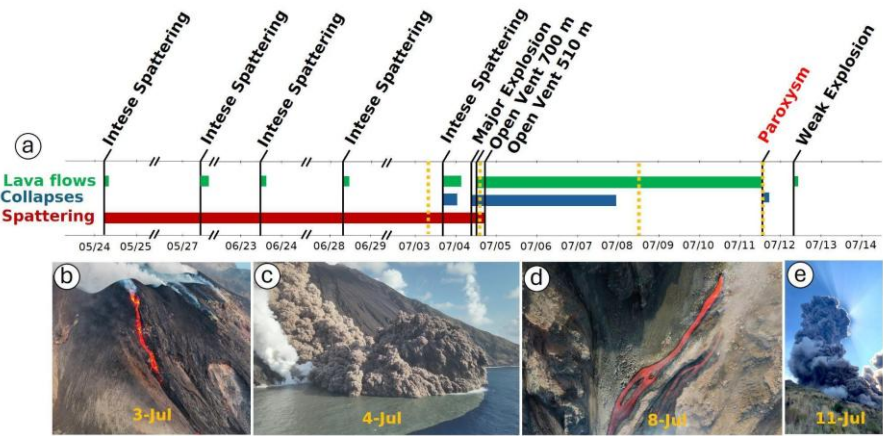


Figure 2: Timeline of the observed surface activity and key visual observations at Stromboli between late May and mid-July 2024. a) Timeline showing the chronology of activity, which marks periods of activity characterized by lava flows (green), collapses (blue) and spattering (red). Significant events are labelled, such as intense spattering, a major explosion on 4 July, opening of new vents, and the paroxysm on 11 July. b-e) Sequence of images gathered at the times indicated by the dashed yellow lines in a). From left to right: spattering activity on 3 July, a PDC event reaching into the sea on 4 July, continued lava flow on 8 July, and the paroxysmal explosion on 11 July (photo “e” courtesy of G. De Rosa - OGS).

137 **3 Geophysical observations**

138 ~~In this study we use data recorded by the geophysical monitoring network deployed and maintained on Stromboli by INGV~~
139 ~~(Fig. 2a; <https://www.ov.ingv.it/index.php/ricercanew/stromboli>). The network includes seismic (ISTR3, ISTR) and~~
140 ~~infrasound sensors (STRA, STRV), as well as seismo-acoustic stations (STR6, STRC, STRE, STRG). An additional infrasound~~
141 ~~sensor, PISA (Gheri et al., 2024), was deployed on 4 July at 13:35 UTC, 35 minutes before the onset of the effusive activity.~~
142 ~~In this study we use data recorded by the geophysical monitoring network deployed and maintained on Stromboli by INGV~~
143 ~~(Fig. 1a). The network includes two seismic broadband stations, equipped with Nanometrics Trillium (0.02–40 s) 3-component~~
144 ~~seismometers and Trident digital acquisition systems (IST3 and ISTR stations), as well as other four broadband station~~
145 ~~employing two GURALP CMG-3ESPC 120 s and two GURALP CMG-40T-60S seismometers (STR6 - STRE and STRC-~~
146 ~~STRG respectively). All the The data recorded are by Guralp seismometers are digitized at 100 Hz and 24-bit resolution with~~
147 ~~Guralp Affinity.~~
148 ~~The infrasound network includes five Chaparral microphones at the stations (STRA, STRC, STRG, STRE and STR6), while~~
149 ~~and a Geco srl sensor at (STRV), and i. Infrasound data are digitized at 100 Hz (only STRA at 50 Hz) and recorded with~~
150 ~~24-bit resolution using Guralp Affinity and Gaia2 digitizers, (<https://eida.ingv.it/>;~~
151 ~~<https://www.ov.ingv.it/index.php/ricercanew/stromboli>). An additional infrasound sensor station, called PISA (Fig. 1a) (Gheri~~
152 ~~et al., 2024), was deployed on 4 July at 13:35 UTC, 35 minutes before the onset of the effusive activity. Pisa was equipped~~
153 ~~with a IST-2018 broadband microphone, and the data were sampled at 100 Hz and digitalized using DIGOS DATA-CUBE³~~
154 ~~24-bit digitizer digital data recorders (e.g., Gheri et al., 2024).~~

156 **3.1 Seismic characterization of unrest and eruptive events**

157 Volcanic tremor is traditionally thought to reflect magma movement within the conduit (McNutt and Nishimura, 2008; Chouet
158 et al., 1997; Ripepe and Gordeev, 1999); at Stromboli, volcanic tremor is routinely monitored by means of the Root Mean
159 Square (RMS) of the continuous seismic signal (54-minut moving window) in the 1-3 Hz frequency band (Giudicepietro et
160 al., 2023). Figure 3a shows RMS tremor amplitude values of the order of 10^{-6} m s^{-1} (recorded at the IST3 site), which correspond
161 to tremor classified by INGV as high. A marked and short-lived increase in seismic RMS tremor amplitude was observed after
162 the major explosion at 12:11 on 4 July (Fig. 3a). During this period, the signal reached unprecedented levels, peaking at 10^{-4}
163 m s^{-1} at 17:00 UTC. Short-lived increases in RMS tremor amplitude values were still noted throughout 5 July, although the
164 RMS amplitudes exhibited an overall decline to values of the order of 10^{-7} m s^{-1} , lower than those recorded at the beginning of
165 July. In the following days (6-11 July), the RMS tremor amplitude was marked by a series of short-duration peaks during lava
166 flow activity. This behaviour changed again on 11 July, when the onset of paroxysmal activity coincided with a new increase
167 in RMS tremor amplitude (Fig. 3a). After the paroxysm, the RMS tremor amplitude decreased again with only sparse and brief
168 intervals of increased amplitudes between 12-13 July (Fig. 3a). From late on 13 July, onwards, the amplitude stabilized around

Commentato [I9]: which refers to the geophysical observations, is too brief and could be expanded with some more detailed information about the instruments used, their characteristics, and the selection of the data for the analysis

ha formattato: Colore carattere: Rosso

Commentato [I10]: Replace by "(Fig. 1a)."

Commentato [I11]: It would be appropriate to clarify at this point (3) the instrumental characteristics as well as in 3.1 justify the frequency ranges analyzed.

ha formattato

ha formattato

ha formattato

ha formattato

Commentato [I12]: I have left some comments and suggestions whose consideration would help the reader to better understand the authors' criteria in the analysis of the continuous tremor and the VLPs

ha formattato: Colore carattere: Rosso

ha formattato: Colore carattere: Rosso

Commentato [I13]: FROM REV3: 4. The authors used terminology seismic tremor and RMS as interchangeable terms e.g. in the caption of Figure 3a, these two terms have different meaning and could lead into confusion. It is also not clear in the text how the authors defined tremor in their observation. Did they use a threshold in the RMS seismic amplitude to separate tremor from the background energy? Was tremor present continuously all the time on 1-18 July or it started and stopped several time?

Commentato [I14]: Please specify the time window used for

ha formattato

Commentato [I15]: Vedere se scrivere sempre figure o fig

Commentato [LZ16]: invece che RMS mettere RMS tremor

Commentato [I17]: Review the superscript edition

Commentato [I18]: It is common to select the HHZ compone

ha formattato: Colore carattere: Rosso

ha formattato

ha formattato: Colore carattere: Rosso

Commentato [I19]: The 12:11 UTC is before, not after, the

ha formattato: Non Evidenziato

ha formattato

Commentato [I20]: Edit superscript

ha formattato

Commentato [I21]: Edit superscript

ha formattato

Commentato [I22]: delete "on" and next ", " after "July"

169 $10^{-7} \text{ m}\cdot\text{s}^{-1}$, indicating that volcanic activity had reduced and returned to background levels. Additional details of the signals
 170 recorded on 4-11 July, are shown in the Supplementary Materials (Fig. 1Sg).

171 The spectrogram in Fig. 3b shows nearly continuous energy in the 2-3 Hz range, typically associated with tremor signals at
 172 Stromboli (Ripepe et al., 1996). Energy levels in this band change throughout the pre-, syn-, and post-explosive activity
 173 periods, reaching a maximum on 4 July following the major explosion, peaking on 4 July (dark red in Fig. 3b) at 17:15 UTC,
 174 following the major explosion, which coincides with the RMS peak (see also Fig. 1Sc). A pulsating phase was observed
 175 from 6-11 July, with another peak during the paroxysm. Explosive activity between 4-11 July, exhibited a broader frequency
 176 range in the 0.5-15 Hz band. It is worth noting that the eruptive event on 4 July was preceded by a high-energy signal in the
 177 narrow frequency band 0.2-0.3 Hz (Fig. 3b). We also observe that this very low-frequency signal was not recorded before the
 178 paroxysm on 11 July. Finally, on 10 July at 05:09 UTC and on 11 July at 02:26 and 15:21 UTC, high-energy signals were
 179 observed around 0.05-0.08 Hz, exhibiting a dispersive spectrum typical of teleseismic events as reported by USGS (for further
 180 information, see: <https://earthquake.usgs.gov/earthquakes/search/>).

181 We have also analysed the occurrence of Very Long Period (VLP) earthquakes that have traditionally been associated with
 182 pressure disturbances and the dynamics of gas-rich magma within fluid-filled structures (Chouet et al., 1997; Chouet et al.,
 183 1999; Marchetti and Ripepe, 2005; Legrand and Pertot, 2022), and one of the main tools used to monitor unrest at Stromboli.

184 VLP events at Stromboli are thought to be generated by a pre-eruptive expansion due to rising pressure in the magma column,
 185 followed by a post-eruptive contraction as pressure decreases. Final oscillations in the VLP signal may be caused by
 186 fluctuations in the conduit or edifice (Legrand and Pertot, 2022). An increase in the frequency of occurrence of these signals
 187 is typically a precursor to periods of elevated eruptive activity (Ripepe et al 2009; Delle Donne et al., 2017). Figure 4a derived
 188 from information sourced from the INGV bulletins (INGV-OE, 2024), provides an overview of the rates of VLP seismicity at
 189 Stromboli between the end of May and mid-July 2024, after the 11 July paroxysm. From May until mid-June, VLP event rates
 190 remained stable, fluctuating around high values between 12 and 19 events/hour. A mean rate of ~13 events/hour is defined,
 191 at Stromboli, as “normal activity” (Ripepe et al., 2008) and it suggests that an efficient degassing mechanism of the magma
 192 column is established (Ripepe et al., 2021b). A significant peak is observed around mid-June, with the number of VLP events
 193 reaching a high of 19 events/hour on June 16. This peak is followed by a slight decrease in event rates, although the number
 194 of events remained elevated compared to previous days. Figure 4b shows the characteristic compression-decompression cycle
 195 of VLP events at Stromboli; this waveform represents the normalized stack of all VLP events with maximum amplitude greater
 196 than $5 \times 10^{-6} \text{ m}\cdot\text{s}^{-1}$ at station STRE. Figure 4c, and more specifically 4d, shows a 1-day filtered (0.03-0.3Hz) seismic record
 197 illustrating the occurrence of VLP events as recorded at station STRE, the closest seismic-acoustic station to the
 198 crater eruptive area, located on the east flank of SdF at 495 m of elevation (see Fig. 1).

199 Before the major explosion on 4 July, we observed a clear drop in the occurrence of VLP events (Fig. 4a) from 10-15 to 7-10
 200 events/hour. The rates of VLP events remained stable until the 11 July paroxysm, peaking again at 12 events/hour on that day.
 201 After the paroxysm, a further decrease in VLP rates was observed with hourly counts ranging from 6 to 10 events.

- ha formattato: Colore carattere: Rosso
- ha formattato: Colore carattere: Rosso, Apice
- ha formattato: Colore carattere: Rosso
- ha formattato: Colore carattere: Rosso, Apice
- ha formattato: Non Evidenziato
- Commentato [123]: From Fig. 1S, it is unclear what the text states about the energy maximum following the major explosion on 4 July. The RMSA between 1 and 3 Hz, understood as proportional to the square root of the energy in that frequency band, shows its maximum during the lava effusion. Maybe the authors could be more specific in their relative description of those amplitudes.
- ha formattato: Colore carattere: Rosso, Barrato
- ha formattato: Colore carattere: Rosso, Barrato
- ha formattato: Colore carattere: Rosso
- Commentato [124]: In risposta alla nota sotto
- ha formattato: Colore carattere: Rosso
- Commentato [125]: It will be helpful to include a definition and some characteristics of VLP events for Stromboli at the beginning of the paragraph that starts in line 153. Please, check the corner frequencies in line 166 because they do not coincide with those in Figure 4.
- Commentato [126]: In line 159 the rate of VLP is described as stable but fluctuating between 12 and 19 events-hour. In line 161, the authors refer to 19 events-hour as a significant peak. So, maybe the stability can be constrained to a narrower rate range.
- ha formattato: Non Evidenziato
- ha formattato: Colore carattere: Rosso, Apice
- ha formattato: Colore carattere: Rosso
- ha formattato: Colore carattere: Rosso, Apice
- ha formattato: Colore carattere: Rosso
- Commentato [127]: In line 166, it could be helpful to point out that STRE is the crater's closest seismic station and that's the reason to choose it for VLP analysis.
- ha formattato: Colore carattere: Rosso
- ha formattato: Colore carattere: Rosso
- ha formattato: Colore carattere: Rosso
- ha formattato: Colore carattere: Rosso

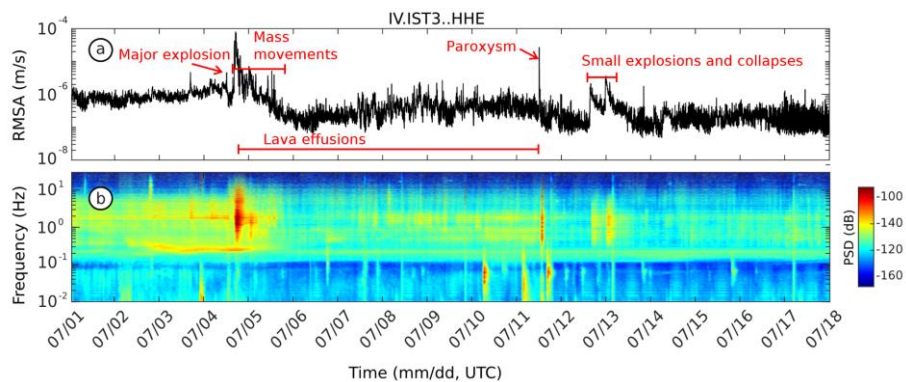
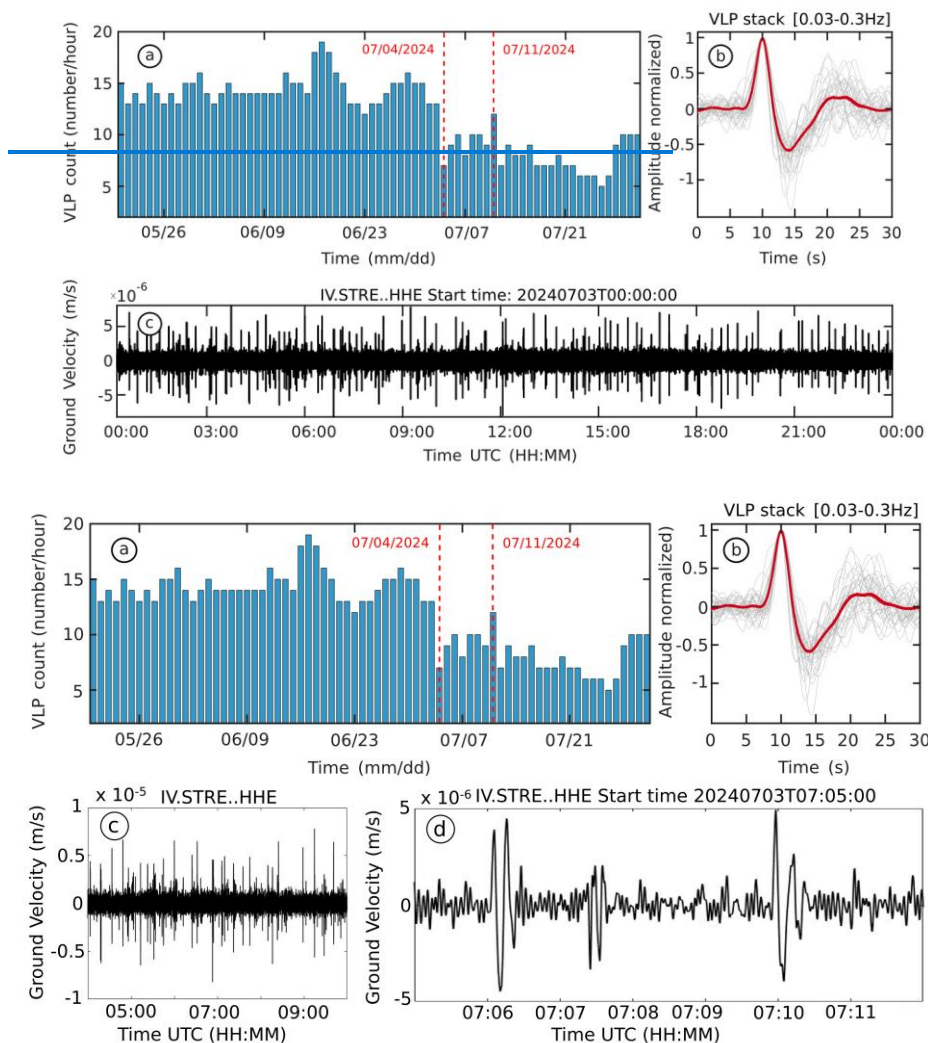


Figure 3: a) Seismic tremor or RMS [tremor amplitude](#) calculated every minute using a moving time window of 5 minutes, within the volcanic tremor frequency band of Stromboli (1-3 Hz), from [July-2 to 18 July](#). b) Spectrogram of the E-component from the IST3 seismic station for the same period.

ha formattato: Non Evidenziato

ha formattato: Colore carattere: Rosso, Non Evidenziato



Formattato: Allineato al centro

Commentato [128]: FROM REV3: 5. Figure 4c is too crowded to show the examples of the recorded LP events. I suggest to plot in a shorter time window to show a clear example of one or few recorded LP waveforms.

ha formattato: Colore carattere: Rosso, Apice

ha formattato: Colore carattere: Rosso

ha formattato: Colore carattere: Rosso, Apice

211 waveforms. c) Continuous waveform recorded at station STRE (EW component) on 3 July 2024, filtered between 0.03-0.3 Hz. d)
212 Extract from c) showing a sequence of VLP events recorded on 3 July over a 7-minute period by the STRE station on the same
213 horizontal component

214 3.2 ~~Infrasound location of the 11 July, 2024 paroxysm~~ ~~characterization of unrest and eruptive events~~

215 We have also analysed infrasound data recorded by the INGV acoustic monitoring network and an additional microphone
216 installed during the period of activity (Fig. 1). The infrasonic record before 4 July, shows a typical background of moderate
217 strombolian activity occasionally interspersed with larger explosions (see Fig. 2Sa). The major explosion on 4 July, generated
218 an infrasonic transient with a pressure of 5 Pa (Fig. 2Sb) at station STR6, ~~~750m from the from the~~ CS crater area. Following
219 this event, a marked decrease in acoustic energy was observed until the 11 July paroxysmal event, which produced infrasonic
220 waves with a peak amplitude of 115 Pa at the STR6 site (~~approximately~~ at ~750 m from the source; see Fig. 1a and Fig.
221 2Sb2Sc).

222 ~~We have used the infrasound records from all operating sensors of the INGV monitoring network on Stromboli and an~~
223 ~~additional temporary microphone (Fig. 2). By analysing infrasound data collected from both the INGV monitoring network~~
224 ~~and temporary microphone, we~~ located the source of the paroxysmal eruption on 11 July, 2024. We employed the RTM-
225 FDTD (Reverse Time Migration - Finite Difference Time Domain) method of Fee et al. (2021), which implements waveform
226 back-projection over a grid of candidate source locations. Travel-times between potential source locations and all stations in
227 the network are calculated via FDTD modeling (Kim and Lees, 2014; Fee et al., 2017; Diaz-Moreno et al., 2019) to account
228 for the effect of topography on the propagation of the acoustic wavefield. In the RTM-FDTD method, waveforms are back-
229 projected and a detector function (e.g., network stack, network semblance) is evaluated for each candidate source, with the
230 detector maximum corresponding to the most likely location. For FDTD calculations of travel-times we employed a UAS-
231 derived Digital Elevation Model (DEM) of the SdF and the summit craters (Civico et al., 2024a,b) areas conducted on the
232 morning of 4 July with initial individual resolutions ranging between 20 and 50 cm/pixel. This DEM was merged with a
233 ~~basemap-reference~~ elevation model (Civico et al., 2021) of the rest of the island, re-sampled, and parsed into a 5x5 m grid for
234 the purpose of FDTD modeling. For FDTD modeling, the source time function was approximated by a Blackman-Harris
235 function with a ~~cutoff frequency of 5 Hz~~ (high enough to include the dominant frequency of the explosion signals, ~~between~~
236 ~~0.2 and 2 Hz~~, while still allowing time-efficient computing) and the acoustic wavefield was propagated along the discretized
237 topography using 15 grid points per wavelength (Wang, 1996). We used a constant sound velocity of 330 ~~m-s⁻¹~~ (estimated
238 from the signal move-out across the network) and a stratified atmosphere model based on density and temperature data obtained
239 from the Reanalysis v5 (ERA5) dataset (see Data and Resources), produced by the European Centre for Medium-Range
240 Weather Forecasts of the Copernicus Climate Change Service. We used data corresponding to the ERA5 grid node closest to
241 Stromboli, at 12:00 on 11 July, 2024 (Coordinated Universal Time, UTC). The inferred source location for the paroxysmal
242 explosion on 11 July, 2024, along with a record section of the infrasound waveforms used and the detector function, are shown
243 in Fig. 5. The location identifies a source located approximately 50m below the rim of the N crater (Fig. 5a) at an elevation of
244 ~685 m. The estimated origin time for the event is 12:08:52 UTC.

Commentato [I29]: in addition to verifying the values mentioned in the text and graphs for the frequency ranges used, I have found some differences between the Pa amplitudes in figures 2Sa, 2Sc, and the text
ha formattato: Colore carattere: Rosso
ha formattato: Colore carattere: Rosso, Barrato

Commentato [I30]: The amplitude of 115 Pa in line 186 coincides with what is seen in Figure 2Sc but not with Figure 2Sa, where the RMSA amplitude for 11 July is lower than those before 4 July. Could the authors check the figures?
ha formattato: Colore carattere: Rosso, Barrato
Commentato [I31]: The statement in line 187 could be simplified because repeats part of what is said in line 181
ha formattato: Colore carattere: Rosso
ha formattato: Colore carattere: Rosso, Barrato
ha formattato: Barrato
ha formattato: Colore carattere: Rosso
ha formattato: Colore carattere: Rosso, Barrato

Commentato [I32]: In Figure 5b the authors show infrasound signals filtered between 0.01 and 15 Hz. Could the authors include a figure with the PPSD of the infrasound signals to support their cutoff frequency selected for the source time function?
ha formattato: Colore carattere: Rosso
ha formattato: Colore carattere: Rosso, Apice
ha formattato: Colore carattere: Rosso

ha formattato: Colore carattere: Rosso, Barrato
ha formattato: Colore carattere: Rosso, Barrato

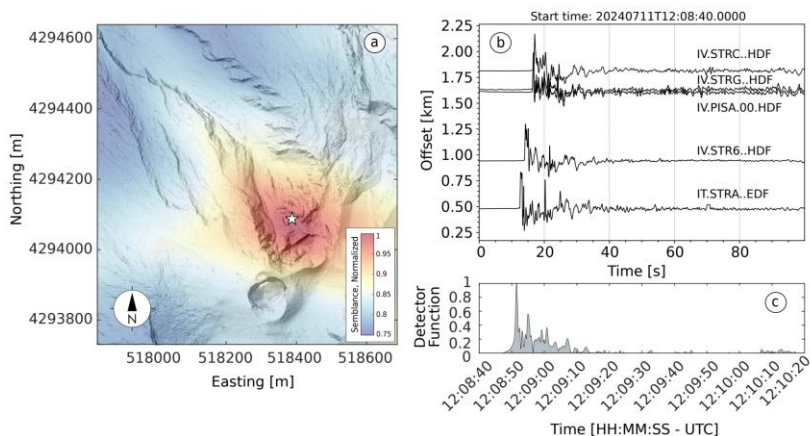


Figure 5: Infrasound location of the 11 July, 2024 paroxysmal event using the RTM-FDTD method (see manuscript for details; DEM of 14 July 14, 2024 from Civico et al. (2024a,b)). a) Map-view of network semblance maximum around the Stromboli crater region. RTM-FDTD semblance location is indicated by a white star; b) record section of the filtered infrasound waveforms (bandpass filter 0.01-15Hz) used for locating the event. The offset corresponds to source-station distance; c) Normalized network detector function (i.e., maximum network semblance amplitude over time).

3.3 Deformation of unrest Tilt and eruptive events

Ground tilt at Stromboli has been frequently been inferred to reflect processes like slug coalescence, slug ascent, and conduit emptying (Marchetti et al., 2009; Genco and Ripepe, 2010; Bonaccorso, 1998). Over the last decade, tilt has become central to real-time monitoring and eruption early warning at Stromboli. Ripepe et al. (2021a), for example, demonstrated the scale invariance of tilt at Stromboli, that is all explosions, regardless of their intensity, follow the same ground inflation-deflation pattern. A significant tilt was reported on 4 July (INGV-OE, 2024). The major explosion at 12:00 UTC was accompanied by a characteristic inflation-deflation pattern (Longo et al., 2024), followed by a pronounced deflation trend that began at 16:20 UTC and continued until 19:50 UTC (INGV-OE, 2024).

Commentato [I33]: lacks the figure mentioned in the text

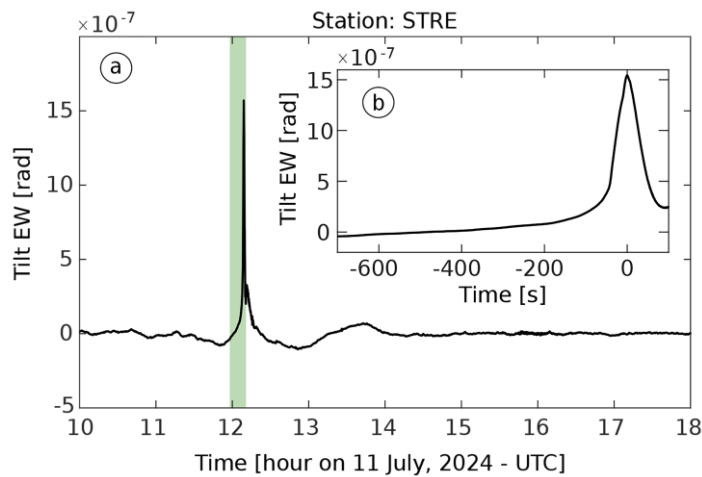


Figure 6: a) Radial tilt recorded by STRE broadband seismic station on 11 July, 2024; b) detail of tilt recorded before the 11 July paroxysm: the signal shows a marked amplitude increases starting ~10 minutes before the onset of the explosion. For the paroxysm on 11 July, 2024 Fig. 6 shows the seismic-derived tilt, reconstructed from the EW horizontal component record at station STRE. The relationship between displacement and tilt sensitivities is a function of the long-period corner frequency of the seismometer used. By applying the a magnification factor (e.g., Aoyama et al. (2008), Genco and Ripepe (2010), and De Angelis and Bodin (2012)), which is constant around the natural period of the seismometer, we were able to convert the seismometer's output from displacement to ground tilt. For the paroxysm on 11 July 2024 Fig. 5 shows the seismic-derived tilt, reconstructed from the EW horizontal component record at station STRE [Aoyama et al. (2008), Genco and Ripepe (2010), and De Angelis and Bodin (2012)]. Slow inflation is observed, starting ~approximately 600 seconds before the explosion (Fig. 5b6b); the seismic-derived tilt sharply accelerates approximately 1 minute before reaching its peak of 1.5 μ rad at the onset of the explosion, followed by rapid deflation. This pattern is consistent with previous observations of tilt at Stromboli before paroxysms and major explosions (e.g. Genco and Ripepe (2010); Ripepe et al. (2021a)). We note that this tilt signal is derived from an individual seismic record, of an instrument that is not likely oriented in the direction radial to the source; for this reason, we will focus on the interpretation of the deformation trend, and will not use the measured tilt amplitude for modelling purposes.

Formattato: Allineato al centro

ha formattato: Tipo di carattere: (Predefinito) +Titoli (Times New Roman), 9 pt, Grassetto, Colore carattere: Rosso

ha formattato: Tipo di carattere: 9 pt, Non Evidenziato

ha formattato: Tipo di carattere: (Predefinito) +Titoli (Times New Roman), 9 pt, Grassetto, Colore carattere: Rosso

ha formattato: Tipo di carattere: 9 pt

ha formattato: Tipo di carattere: (Predefinito) +Titoli (Times New Roman), 9 pt, Grassetto, Colore carattere: Rosso

ha formattato: Tipo di carattere: 9 pt

ha formattato: Tipo di carattere: 9 pt, Non Evidenziato

ha formattato: Tipo di carattere: 9 pt, Non Evidenziato

Formattato: Interlinea: singola

ha formattato: Tipo di carattere: 9 pt, Non Evidenziato

ha formattato: Tipo di carattere: 9 pt, Non Evidenziato

ha formattato: Tipo di carattere: 9 pt, Non Evidenziato

ha formattato: Tipo di carattere: 9 pt

ha formattato: Tipo di carattere: (Predefinito) +Titoli (Times New Roman), 9 pt, Grassetto, Colore carattere: Rosso

Commentato [I34]: Figure 5 shows infrasound records and location solution. The Figure 3S shows velocity record of STRE HHE. Would the authors verify the shown information? I can't make comments on lines 224 to 231

Commentato [I35]: FROM REV3: 7. The authors did not write how they derived tilt from seismic data and only wrote the citations from the former publications which used the same method. For the completeness of the paper, this step needs to be included.

277 **4 Discussion**

278 In this manuscript we have presented geophysical data recorded between early and mid-July 2024 at Stromboli; the period of
279 unrest included a major explosion on 4 July, significant collapse activity in the N summit crater area, emplacement of lava
280 flows, and a paroxysmal event on 11 July. Surface activity at Stromboli intensified late in May with a marked increase in the
281 occurrence of Strombolian explosions, the onset of effusive activity from SdF, and increasing volcanic tremor. Using multi-
282 parameter observations~~Through multidisciplinary approach, we reconstructed the chronology~~observed a time evolution of the
283 eruptive activity, which culminated with into the paroxysmal explosion on 11 July, 2024.

284
285 **4.1 Eruptive activity during the first week of July, 2024.**

286 ~~In the first week of~~ Early in July, we observed a steady increase in volcanic tremor reaching unprecedented amplitudes on 4
287 July, (see Fig. 3a and Fig. 1S). Volcanic tremor at Stromboli has typically been linked to the coalescence of gas bubbles from
288 layers of smaller bubbles and their ascent along the shallower conduit (McNutt et al., 2008; Chouet et al., 1997; Ripepe et al.,
289 1999), suggesting that variations in tremor intensity are controlled by changes in gas flow within the conduit.
290 It has been frequently speculated that an increase in volcanic tremor reflects an increase in the volume of gas within the magma
291 (Ripepe et al., 1996), which in turn is linked to a higher occurrence of explosions at the top of the magma column. Field
292 observations of increasing spattering in early July (Fig. 1) support a model of increased surface activity linked to the ascent of
293 gas-rich magma within the shallow conduit. The spattering activity, observed at the start of our study period, represents an
294 intensified form of puffing. Spattering activity results from the quasi-continuous bursting of small gas pockets within a bubbly
295 flow regime, which generates pyroclasts fragments (Rosi et al., 2013). This activity typically marks the initial stages of unrest
296 and eruption at Stromboli, where gas-rich magma is being actively degassed through continuous explosive bursts (Del Bello
297 et al., 2012). The high rates of VLP events observed during the same period further support the hypothesis of gas-rich magma
298 migration within the shallow plumbing system. These events are traditionally ~~associated with~~ linked to the rapid expansion of
299 gas ~~bubbles~~ slugs rising through the liquid melt in the shallow conduit (Chouet et al., 2003; James et al., 2006); more recently
300 (Ripepe et al., 2021) suggested that VLP waveforms at Stromboli are generated at the top of the magma column, mainly after
301 the onset of Strombolian explosions; they showed that the occurrence of VLP event can be linked to explosive magma
302 decompression in the uppermost ~250 m of the conduit. The recorded VLP events showed similar waveforms (Fig. 4b)
303 suggesting a stable source mechanism and location; locations in the shallow parts of the conduit can be linked to magma
304 accumulation at a shallow depth, close to the surface. While the number of VLP events did not show any significant variation
305 before the major explosion on 4 July, volcanic tremor increased slowly but steadily (Fig. 3a). Coinciding with strong ground
306 deflation after the major explosion (INGV-OE, 2024), volcanic tremor reached an unprecedented peak amplitude of $\sim 8 \times 10^{-5}$
307 m s^{-1} at ~17:00 UTC associated with the opening of a new effusive vent at ~510 m elevation within SdF (Fig. 2a) and the
308 occurrence of numerous mass wasting events linked to collapse activity within the lower N crater area and upper section of
309 SdF. We suggest that these signals reflect the emptying of the shallowest parts of the conduit system and the overall lowering

Commentato [I36]: Delete "by"

- ha formattato: Colore carattere: Rosso
- ha formattato: Colore carattere: Rosso, Apice
- ha formattato: Colore carattere: Rosso
- ha formattato: Colore carattere: Rosso, Apice

310 of the magma level within the shallow volcano plumbing reflected in the opening of new effusive vents at progressively lower
311 elevations. The transition between explosive and effusive regimes was also marked by a clear decrease in the occurrence of
312 VLP events (Fig. 4), and a migration of their source deeper within the conduit (as reported by the automatic seismic monitoring
313 of INGV- Osservatorio Vesuviano: ~~(<http://eolo.ov.ingv.it/eolo/3>)~~ and as already observed during past unrest by Ripepe et al.,
314 (2015)). This contrasts with the flank eruptions of 2007 and 2014 (Ripepe et al., 2009; ~~Ripepe et al., 2015~~) when VLP rates
315 remained high during effusion; in July, 2024 it appears that effusion reduced the overall explosivity through progressive
316 degassing of the shallow magma, rather than recalling fresh, gas-rich, magma from depth. The new effusive regime, indeed,
317 was characterized by a substantial lack of Strombolian explosive activity at the surface between 4-11 July, as observed in the
318 field by our research team. The quasi-continuous collapse activity, observed from 13:00 UTC on 4, July, appeared to be linked
319 to instabilities in the crater area around newly created vents; this instability persisted in the following days, with the number
320 of events peaking on 5 July-5 (83 recorded occurrences recorded in a single day (INGV-OE, 2024)). The collapse activity
321 recorded along the N crater rim, adjacent to the SdF, resulted in significant changes to the morphology of this sector of the
322 volcanic edifice (Fig. 67).

323
324
325 **4.2 Eruptive activity during the second week of July, 2024.**
326 The effusive regime, that began on 4 July, ended During the study period, we also collected UAS data and compiled very high-
327 resolution repeat DEMs (0.2-0.5 m/pixel), which allowed quantifying topographical changes via DEM differencing. The
328 difference between DEMs on 4, July, (morning; Civico et al., 2025) and 14 July (Civico et al., 2024a,b) 14 is shown in Fig.
329 7e7e. The data processing methodology follows the procedures described in Civico et al. (2022, 2024a). The most notable
330 morphological variations were observed in the afternoon of 4 July, while the paroxysm on 11 July did not lead to significant
331 changes.

332 The summit craters were affected by loss of material due to the opening of two eruptive vents at approximately 700 and 500
333 m a.s.l.. While the CS crater sector showed a roughly circular shape crater floor deepening of about 84 m, the N sector was
334 affected by the complete dismantling of its northern rim and external slope, marking the deepest morphological change
335 occurred at the summit craters in the last decades, with a maximum difference in altitude of 109 m. The total volume loss
336 recorded in the summit craters sector was estimated at 3.3 Mm³ (Civico et al., 2024a).

ha formattato: Colore carattere: Rosso

ha formattato: Colore carattere: Rosso

ha formattato: Colore carattere: Rosso

Codice campo modificato

Commentato [I37]: Does this work prove the migration of VLP sources or are the authors citing Ripepe et al., 2015? In line 188 the authors point out they have located just the explosion on 11 July

ha formattato: Colore carattere: Rosso

ha formattato: Colore carattere: Rosso, Barrato

ha formattato: Colore carattere: Rosso

ha formattato: Colore carattere: Rosso, Barrato

ha formattato: Colore carattere: Rosso

ha formattato: Tipo di carattere: Grassetto

ha formattato: Tipo di carattere: Grassetto

Formattato: Normale

Commentato [I38]: Figure 6c

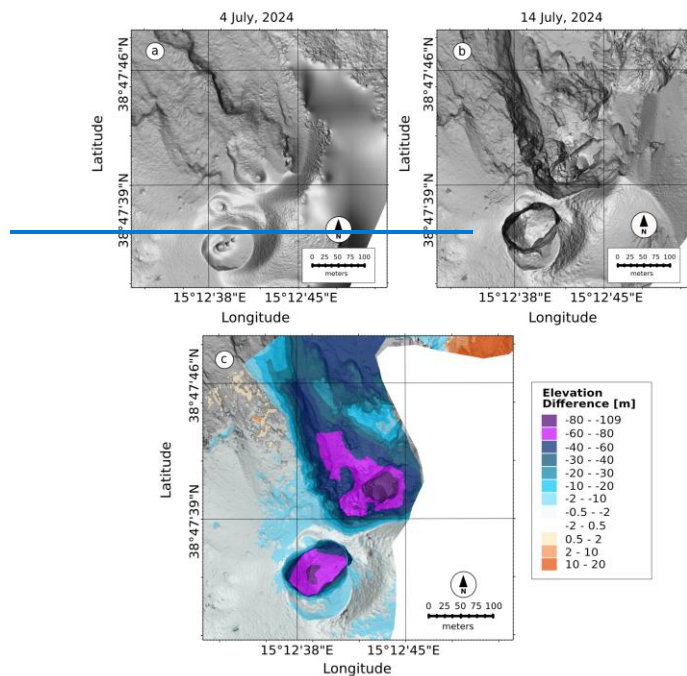


Figure 6: Multidirectional hillshades of Stromboli's crater area: a) 4, July 2024 (Civico et al., 2024c5), b) July 14, 2024 (Civico et al., 2024a,b), c) map of elevation difference (Dem of Differences) highlighting morphological changes occurred between 4 and 14 July, 2024. Purple areas indicate material loss, whereas orange areas indicate material gain.

Unlike the summit craters, the subaerial portion of the SdF slope was affected by both accumulation and erosion processes. Here, the main loss of material (2.74 Mm^3 ; Civico et al., 2024a) was localized along the canyon formed in October 2022 (Di Traglia et al., 2024), which has widened and deepened during the July 2024 eruption. Accumulation processes instead were mainly due to PDC and lava flow deposits, localized in the northeastern sector of the slope. The maximum accumulation of lavas occurred at the new lava delta (maximum difference in altitude of 45 m), located in the center of the SdF shoreline.

4.2 Eruptive activity during second week of July, 2024.

The effusive regime ended with the occurrence of the paroxysmal explosion on 11, July. The explosion generated an infrasonic pressure of 115 Pa at station STR6 with an associated VLP peak amplitude reaching of $5.8 \times 10^{-5} \text{ ms}^{-1}$ 10.5 m s^{-1} (see Fig.

ha formattato: Colore carattere: Rosso

Commentato [139]: There is only one Civico et al., 2024 in References.

Commentato [140]: Area in Figure 6 doesn't include this lava delta. So, please cite Civico et al., 2024

350 3S). ~~An~~The associated ash plume reached a height of 5 km above the vent, and pyroclastic flows moved down the SdF. After
351 that, volcanic activity reduced its intensity, ~~accompanied by showing~~ low levels of tremor and VLP events; ~~although the~~ tremor
352 increased again on 12 July, associated with ~~emplacement of~~ a small lava flow.

353 The eruptive crisis of July 2024, culminating into the 11 July paroxysm, is consistent with previous eruptions at Stromboli,
354 such as those in April 2003, March 2007, and July-August 2019. The ~~observations that we have presented in this~~
355 ~~manuscript data discussed above~~ can be used to inform a conceptual model of the entire sequence of processes responsible for
356 the observed surface and eruptive activity, within the framework of previous studies (e.g., James et al., 2006; Chouet et al.,
357 2008; Del Bello et al., 2012; Suckale et al., 2015; McKee et al., 2022).

358 ~~The spattering activity, observed at the start of our study period, represents an intensified form of puffing. Spattering activity~~
359 ~~results from the quasi-continuous bursting of small gas pockets within a bubbly flow regime, which generates pyroclasts~~
360 ~~fragments (Rosi et al., 2013). This activity typically marks the initial stages of unrest and eruption at Stromboli, where gas-~~
361 ~~rich magma is being actively degassed through continuous explosive bursts (Del Bello et al., 2012).~~ At the more explosive end
362 of the spectrum of Strombolian activity major explosions and paroxysms are often explained invoking the "slug model" (James
363 et al., 2006; Chouet et al., 2008; Del Bello et al., 2012). In this model, gas bubbles (slugs) form deeper in the magma column
364 and gradually coalesce as they rise through the conduit due to an increase of the magma viscosity. As gas slugs ascend, they
365 expand due to ~~the~~ decreasing ~~confining~~ pressure and eventually reach the surface. When they burst at the top of the magma
366 column, they release gas explosively, fragmenting the magma and producing pyroclasts and feeding ash plumes of varying
367 sizes. After the major explosion on 4 July, an effusive regime was established, characterized by lava flows, during which more
368 degassed magma was erupted. Following the initial explosive activity driven by gas slugs, we infer that the transition to ~~the~~
369 effusive regime ~~was~~ controlled by depressurization of the shallow plumbing system similar to ~~the model of~~ Ripepe et al.
370 (2017). The depressurization of the system caused by the initial explosive activity allowed magma to flow, and reach the
371 surface forming lava flows, without further explosive activity. As the shallow volcanic conduit progressively emptied it ~~leads~~
372 to structural instability, causing collapses and landslides along the SdF.

373 According to Ripepe et al. (2017), the emptying of the conduit creates a "vacuum" effect that draws more gas-rich magma
374 from deeper within the system. As volatile-rich magma rises and ~~experiences encounters~~ lower pressures, ~~activity can be~~
375 ~~triggered, sometimes it can lead to explosive eruptions;~~ resulting in a paroxysmal event. The dynamics of the 11 July
376 paroxysmal explosion ~~shared similarities displayed similar trends~~ across seismic, acoustic, and deformation parameters ~~with~~
377 ~~past events compared to the others~~ (Genco and Ripepe, 2010; Ripepe et al., 2021a). This consistency further validates the
378 established models ~~of activity and Stromboli of Strombolian activity~~, where the largest explosions and energetic events, such
379 as paroxysms, are driven by the same source mechanism. The scale-invariant conduit dynamics of ground deformation
380 demonstrate that inflation amplitude and duration scale directly with the magnitude of the explosion (Ripepe et al., 2021a).

381 Ground deformation observed on 11 July (Fig. 56) follows the same exponential inflation pattern as seen in previous
382 paroxysms (Ripepe et al., 2021a). This ~~behavior~~behaviour is typically explained by bubble dynamics, where the pressure on
383 the conduit walls increases due to the rapid volumetric expansion of gas in highly vesiculated magma. As gas rises and expands,

ha formattato: Colore carattere: Rosso, Barrato

ha formattato: Colore carattere: Rosso, Barrato

Commentato [I41]: The Figure with ground deformation is missing

ha formattato: Colore carattere: Rosso, Barrato

ha formattato: Colore carattere: Rosso

ha formattato: Colore carattere: Rosso, Non Evidenziato

384 moreover, it pushes the magma column toward the surface, often leading to precursory lava emissions from the vent. Ground
385 deformation is likely caused by a combination of increasing magma static pressure and the pressurization of degassed magma
386 at the top of the column, driven by the exponential expansion of the gas phase~~growth of gas~~. When the pressure applied by
387 the gas-rich magma exceeds the tensile strength of the viscous magma plug, fragmentation occurs, resulting in the explosive
388 release of gas and pyroclastic material (e.g. paroxysm). Another possible mechanism, proposed by Suckale et al. (2016) and
389 McKee et al., (2022) suggests that the explosion is triggered by the rapid expansion and release of gas when a partial rupture
390 occurs in the plug at the top of the magma column.

391
392

393 **4.3 Morphological changesing of the crater area caused by the explosive activity.**

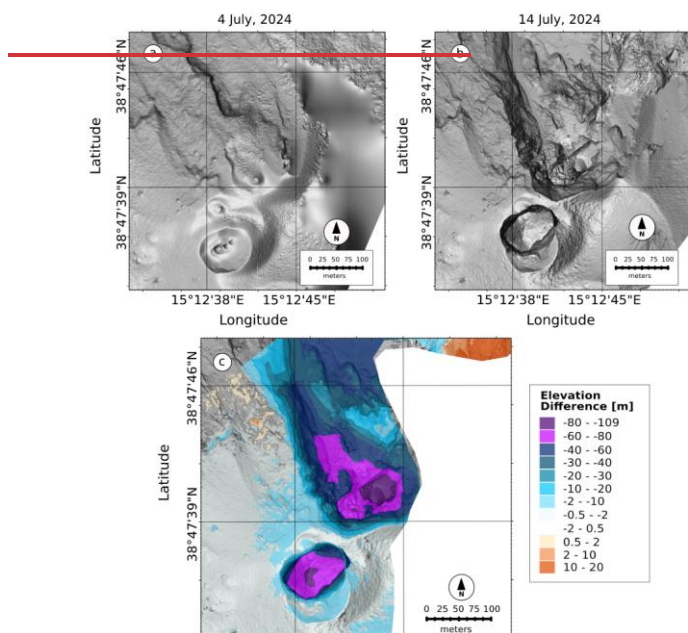
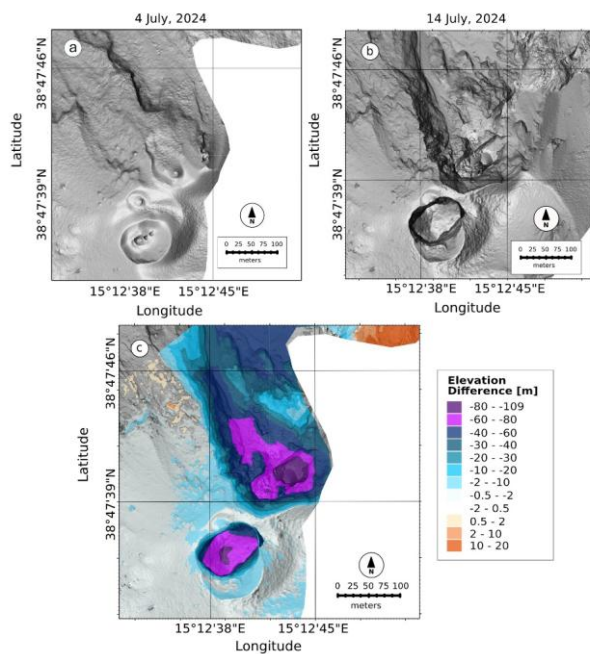
394 During the study period, we also collected UAS data and compiled very high-resolution repeat DEMs (0.2-0.5 m/pixel), which
395 allowed quantifying topographical changes via DEM differencing. The difference between DEMs on 4 July (morning; Civico
396 et al., 2025) and 14 July (Civico et al., 2024a,b) is shown in Fig. 7c. The data processing methodology follows the procedures
397 described in Civico et al. (2022, 2024a). The most notable morphological variations were observed in the afternoon of 4 July,
398 while the paroxysm on 11 July did not lead to significant changes.
399 The summit craters were affected by experienced loss of material due to the opening of two eruptive vents at approximately
400 700 and 500 m a.s.l.. While the CS crater sector showed a roughly circular-shape -crater floor deepening of about 84 m, the N
401 sector was affected by the complete dismantling of its northern rim and external slope, marking the deepest morphological
402 change occurredobserved at the summit craters in the last decades, with a maximum difference in altitude of 109 m. The total
403 volume loss recorded in the summit craters sector was estimated at 3.3 Mm³ (Civico et al., 2024a).

ha formattato: Tipo di carattere: Grassetto

ha formattato: Tipo di carattere: Grassetto, Colore
carattere: Automatico

Commentato [lu42]: Figure 6c

ha formattato: Non Evidenziato



405 Figure 7: Multidirectional hillshades plots of Stromboli's crater area: a) 4 July, 2024 (Civico et al., 2025), b) 14 July, 2024 (Civico et
406 al., 2024a,b), c) map of elevation difference (Dem of Differences) highlighting morphological changes occurred between 4 and 14
407 July, 2024. Purple areas indicate material loss, whereas orange areas indicate material gain.

408 Unlike the summit craters, the subaerial portion of the SdF slope was affected by both accumulation and erosion processes.
409 Here, the main loss of material (2.74 Mm³; Civico et al., 2024a) was localized along the canyon formed in October 2022 (Di
410 Traglia et al., 2024), which has widened and deepened during the July 2024 eruption. On the other hand, Accumulation
411 processes instead were mainly due to PDC and lava flow deposits, localized within in the northeastern sector of the
412 slopededifice. [The maximum accumulation of lavas occurred at the new lava delta (maximum difference in altitude of 45 m).
413 located in the center of the SdF shoreline (Civico et al., 2024a).]

Commentato [lu43]: There is only one Civico et al., 2024 in References.

Commentato [lu44]: Area in Figure 6 doesn't include this lava delta. So, please cite Civico et al., 2024

415 **5 Conclusion**

416 The eruptive activity at Stromboli starting from 4₂ July, and culminating with a paroxysm on 11₂ July, 2024, with the
417 paroxysm,provides a comprehensive case study of explosive volcanism at open-conduit volcanoes, thus and offering valuable
418 additional insights into its causative processes and mechanism, and proofs for already-existing source models.

419 The July 2024 paroxysm was preceded by a prolonged phase of heightened activity, characterized by increased volcanic
420 tremor and VLP events. The high-elevated levels of seismicity, combined with observed crater rim collapses and lava flows,
421 suggests a progressive destabilization of the volcanic edifice. In particular, the major explosion on 4₂ July, and the subsequent
422 paroxysm on 11₂ July highlight highlights the role of magma gas dynamics, where increased gas volumes and pressure led to
423 significant eruptive events.

424 Analysis of the seismic recordsSeismic analysis reveals that the volcanic tremor intensity is linked to gas-rich magma
425 movement, reaching in this eruptive sequence unprecedented values at Stromboli. However, the variability in VLP events
426 indicates that, while useful for monitoring overall volcanic unrest, these signals alone may not serve as reliable precursors
427 for major explosive events. Instead, the combined analysis of different geophysical parameters, including ground deformation,
428 proved crucial for early warning and forecasting as previously suggested by Ripepe et al. (2021a).

429 Ground deformation patterns, specifically the inflation-deflation cycle observed before explosions, align with previous studies,
430 confirming that such patterns reflect the occurrence of imminent explosions regardless of their magnitude. The exponential
431 inflation observed before the paroxysm, caused by gas expansion and the rise of slugs within the magma column, is the same
432 as in other paroxysmal events at Stromboli, supporting the already-proposed source mechanism models for explosive events.

433 Through UAS data, Civico et al. (2024a) were able to estimate a total volume loss of about 6.0 Mm³ involved after the
434 gravitational mass collapses occurred on 4 and 11 July. The partial collapses generated a reshaping of the summit craters area
435 as well as a deepening 2022 canyon along SdF, thus increasing the flank instability.

436 In conclusion, our results demonstrate how geophysical, visual observation and UAS-derived topographic data could offer
437 valuable-new, valuable, insights for tracking and characterizing the processes that control the onset of volcanic explosive

ha formattato: Colore carattere: Rosso, Barrato

ha formattato: Colore carattere: Rosso, Barrato

ha formattato: Colore carattere: Rosso, Barrato

ha formattato: Colore carattere: Rosso, Barrato

ha formattato: Colore carattere: Rosso

ha formattato: Colore carattere: Rosso, Apice

activity at Stromboli and other similar volcanoes. We suggest that multi-parameter volcano monitoring will lead to further significant advances in volcanic hazard mitigationthe volcanic explosive phenomena as well as the partial collapses of the summit craters due to the flank instability. This multiparametric monitoring approach could lead to significant advancements in reducing volcanic hazards at Stromboli.

Data availability

The seismic waveform data used in this study are from thefrom all the stations are part of INGV seismic network. The All data are publicly available at from EIDA Italia (<https://eida.ingv.it/>). The infrasound data are available upon request from the INGV - Osservatorio Vesuviano or direct enquiry to the authors of this manuscript. The infrasound data are collected from PISA station are available at <https://doi.org/10.5281/zenodo.14245572>.

Author contribution

L.Z., S.D.A. and P.S. wrote the research proposals that funded the installation and maintenance of the infrasound array and UAS, designed the field experiment, and financially supported this publication. L.Z. and S.D.A. tested the infrasonic equipment, organized fieldwork and participated in the original design of the experiment. L.Z., S.D.A., R.C., T.R. contributed to assembling the final multiparametric dataset and tested its quality and retrieval. L.Z., R.C. and T.R. installed and maintained the equipment during the field acquisition. L.Z., S.D.A. and D.G. performed analyses of infrasound data, seismic and tilt data, and prepared all figures. R.C. and T.R. acquired and analysed the UAS images. L.Z., D.G. and S.D.A. jointly wrote the initial draft of the manuscript and all authors contributed to review and edit the final version.

Competing interests

The authors declare that they have no conflict of interest.

Acknowledgements

INGV Project ‘Pianeta Dinamico (Dynamic Planet) - Working Earth’: Geosciences For The Understanding The Dynamics Of The Earth And The Consequent Natural Risks - “Dynamo - DYNAMics of eruptive phenoMena at basaltic vOlcanoes” (<https://progetti.ingv.it/it/pian-din/dynamo#project-info>).

INGV Departmental Strategic Project “UNO - UNderstanding the Ordinary to forecast the extraordinary: An integrated approach for studying and interpreting the explosive activity at Stromboli volcano” (<https://progetti.ingv.it/it/uno-stromboli>).

L.Z., D.G., S.D.A., R.C., T. R. and P.G. are supported by the grant "Progetto INGV Pianeta Dinamico" - Sub-project VT_DYNAMO 2023 - code CUP D53J19000170001 - funded by Italian Ministry MIUR (“Fondo Finalizzato al rilancio degli investimenti delle amministrazioni centrali dello Stato e allo sviluppo del Paese”, legge 145/2018).

We are indebted to all the INGV colleagues who have contributed to the monitoring efforts on Stromboli during July 2024 and the ones involved in the surveillance and network maintenance activities, to Maria Zagari (Italian Civil Aviation Authority - ENAC) for her help in issuing new NOTAMs during the emergency, and to Giuseppe De Rosa, Istituto Nazionale di Oceanografia e di Geofisica Sperimentale (OGS) for providing the photo of the 11 July paroxysm in Fig. 1. The contents of this article represent the authors' ideas and do not necessarily correspond to the official opinion and policies of the Dipartimento della Protezione Civile - Presidenza del Consiglio dei Ministri. We are grateful to the "Gruppo monitoring dei colleghi di INGV - Osservatorio Vesuviano" of INGV, Osservatorio Vesuviano (Italy), for their support in the data management.

Financial support

This work was supported by the grant "Progetto INGV Pianeta Dinamico" -Sub-project VT_DYNAMO 2023- code CUP D53J19000170001 - funded by Italian Ministry MIUR ("Fondo Finalizzato al rilancio degli investimenti delle amministrazioni centrali dello Stato e allo sviluppo del Paese", legge 145/2018) and by INGV Departmental Strategic Project "UNO - Understanding the Ordinary to forecast the extraordinary: An integrated approach for studying and interpreting the explosive activity at Stromboli volcano".

References

Aiuppa, A., Burton, M., Caltabiano, T., Giudice, G., Guerrieri, S., Liuzzo, M., and Salerno, G.: Unusually large magmatic CO₂ gas emissions prior to a basaltic paroxysm, *Geophys. Res. Lett.*, 37, <https://doi.org/10.1029/2010GL044997>, 2010.

Andronico, D., Del Bello, E., D’Orlando, C., Landi, P., Pardini, F., Scarlato, P., and Valentini, F.: Uncovering the eruptive patterns of the 2019 double paroxysm eruption crisis of Stromboli volcano, *Nat. Commun.*, 12, <https://doi.org/10.1038/s41467-021-23349-4>, 2021.

Bertagnini, A., Métrich, N., Landi, P., and Rosi, M.: Stromboli volcano (Aeolian Archipelago, Italy): An open window on the deep-feeding system of a steady state basaltic volcano, *J. Geophys. Res. Solid Earth*, 108, <https://doi.org/10.1029/2002JB002146>, 2003.

Bonaccorso, A.: Evidence of a dyke-sheet intrusion at Stromboli Volcano inferred through continuous tilt, *Geophys. Res. Lett.*, 25, <https://doi.org/10.1029/98GL00766>, 1998.

Burton, M., Allard, P., Murè, F., and La Spina, A.: Magmatic gas composition reveals the source depth of slug-driven Strombolian explosive activity, *Science*, 317, <https://doi.org/10.1126/science.1141900>, 2007.

Calvari, S., Spampinato, L., and Lodato, L.: The 5 April 2003 vulcanian paroxysmal explosion at Stromboli volcano (Italy) from field observations and thermal data, *J. Volcanol. Geotherm. Res.*, 149, <https://doi.org/10.1016/j.jvolgeores.2005.09.008>, 2006.

Commentato [145]: Please review this sentence.

ha formattato: Colore carattere: Rosso, Barrato

Calvari, S., Spampinato, L., Bonaccorso, A., Oppenheimer, C., Rivalta, E., and Boschi, E.: Lava effusion—A slow fuse for paroxysms at Stromboli volcano? *Earth Planet. Sci. Lett.*, <https://doi.org/10.1016/j.epsl.2011.03.005>, 2011.

Calvari, S., and Nunnari, G.: Statistical insights on the eruptive activity at Stromboli volcano (Italy) recorded from 1879 to 2023, *Remote Sensing*, 15, <https://doi.org/10.3390/rs15174298>, 2023.

Caricchi, L., Montagna, C. P., Aiuppa, A., Lages, J., Tamburello, G., and Papale, P.: CO₂ flushing triggers paroxysmal eruptions at open conduit basaltic volcanoes, *J. Geophys. Res.: Solid Earth*, 129, <https://doi.org/10.1029/2023JB02561>, 2024.

Chouet, B., Saccorotti, G., Martini, M., Dawson, P., De Luca, G., Milana, G., and Scarpa, R.: Source and path effects in the wave fields of tremor and explosions at Stromboli Volcano, Italy, *J. Geophys. Res.: Solid Earth*, 102, <https://doi.org/10.1029/96JB03395>, 1997.

Chouet, B., Dawson, P., Ohnminato, T., Martini, M., Saccorotti, G., Giudicepietro, F., De Luca, G., Milana, G., and Scarpa, R.: Source mechanisms of explosions at Stromboli Volcano, Italy, determined from moment-tensor inversions of very-long-period data, *J. Geophys. Res.: Solid Earth*, 108, <https://doi.org/10.1029/2002JB001919>, 2003.

Chouet, B., Dawson, P., and Martini, M.: Shallow-conduit dynamics at Stromboli Volcano, Italy, imaged from waveform inversions, *Geol. Soc. London, Special Publications*, 307, <https://doi.org/10.1144/SP307.5>, 2008.

Colò, L., Ripepe, M., Baker, D. R., and Polacci, M.: Magma vesiculation and infrasonic activity at Stromboli open conduit volcano, *Earth Planet. Sci. Lett.*, 292, <https://doi.org/10.1016/j.epsl.2010.01.041>, 2010.

Civico, R., Ricci, T., Scarlato, P., Andronico, D., Cantarero, M., Carr, B. B., De Beni, E., Del Bello, E., Johnson, J. B., Kueppers, U., Pizzimenti, L., Schmid, M., Strehlow, K., and Taddeucci, J.: Unoccupied Aircraft Systems (UASs) Reveal the Morphological Changes at Stromboli Volcano (Italy) before, between, and after the 3 July and 28 August 2019 Paroxysmal Eruptions, *Remote Sensing*, 13, <https://doi.org/10.3390/rs13010141>, 2021.

Civico, R., Ricci, T., Cecili, A., and Scarlato, P.: High-resolution topography reveals morphological changes of Stromboli volcano following the July 2024 eruption, *Sci. Data*, 11, 1219, <https://doi.org/10.1038/s41597-024-04098-y>, 2024a.

Civico, R., Ricci, T., Scarlato, P.: High-Resolution SfM Topography of Stromboli volcano (Italy), 14 July 2024, *OpenTopography*, <https://doi.org/10.5069/G9S75DJH>, 2024b. Accessed: 2025-02-05

Civico, R., Ricci, T., Scarlato, P.: SfM Topography of Stromboli volcano (Italy), 04 July 2024 – crater terrace, *OpenTopography*, <https://doi.org/10.5069/G9WW7FWN> <https://doi.org/10.5069/G9T151WP>, 2025. Accessed: 2025-02-05

D’Auria, L., Giudicepietro, F., Martini, M., and Peluso, R.: Seismological insight into the kinematics of the 5 April 2003 vulcanian explosion at Stromboli volcano (southern Italy), *Geophys. Res. Lett.*, 33, <https://doi.org/10.1029/2005GL025502>, 2006.

De Angelis, S., and Bodin, P.: Watching the Wind: Seismic Data Contamination at Long Periods due to Atmospheric Pressure-Field-Induced Tilting, *Bull. Seismol. Soc. Am.*, 102, <https://doi.org/10.1785/0120110245>, 2012.

528 Del Bello, E., Llewellyn, E. W., Taddeucci, J., Scarlato, P., and Lane, S. J.: An analytical model for gas overpressure in slug-
529 driven explosions: Insights into Strombolian volcanic eruptions, *J. Geophys. Res.: Solid Earth*, 117(B2),
530 <https://doi.org/10.1029/2011JB008747>, 2012.

531 Diaz-Moreno, A., Iezzi, A. M., Lamb, O. D., Fee, D., Kim, K., Zuccarello, L., and De Angelis, S.: Volume Flow Rate
532 Estimation for Small Explosions at Mt. Etna, Italy, From Acoustic Waveform Inversion, *Geophys. Res. Lett.*, 46,
533 <https://doi.org/10.1029/2019GL084159>, 2019.

534 Di Traglia, F., Berardino, P., Borselli, L., Calabria, P., Calvari, S., Casalbore, D., et al.: Generation of deposit-derived
535 pyroclastic density currents by repeated crater rim failures at Stromboli Volcano (Italy), *Bull. Volcanol.*, 86,
536 <https://doi.org/10.1007/s00445-024-01516-0>, 2024.

537 Delle Donne, D., Tamburello, G., Aiuppa, A., Bitetto, M., Lacanna, G., D'Aleo, R., and Ripepe, M.: Exploring the explosive-
538 effusive transition using permanent ultraviolet cameras, *J. Geophys. Res.: Solid Earth*, 122(6), 4377–4394,
539 <https://doi.org/10.1002/2017JB014027>, 2017.

540 European Centre for Medium-Range Weather Forecasts (ECMWF), ECMWF Reanalysis v5. Available at:
541 <https://www.ecmwf.int/en/forecasts/dataset/ecmwf-reanalysis-v5>. Access date: 21 July 2024.

542 Fee, D., Izbekov, P., Kim, K., Yokoo, A., Lopez, T., Prata, F., Kazahaya, R., Nakamichi, H., and Iguchi, M.: Eruption mass
543 estimation using infrasound waveform inversion and ash and gas measurements: Evaluation at Sakurajima Volcano, Japan,
544 *Earth Planet. Sci. Lett.*, 480, <https://doi.org/10.1016/j.epsl.2017.09.043>, 2017.

545 Fee, D., Toney, L., Kim, K., Sanderson, R. W., Iezzi, A. M., Matoza, R. S., De Angelis, S., Jolly, A. D., Lyons, J. J., and
546 Haney, M. M.: Local Explosion Detection and Infrasound Localization by Reverse Time Migration Using 3-D Finite-
547 Difference Wave Propagation, *Front. Earth Sci.*, 9, <https://doi.org/10.3389/feart.2021.640202>, 2021.

548 Francalanci, L., Tommasini, S., and Conticelli, S.: The volcanic activity of Stromboli in the 1906–1998 AD period:
549 mineralogical, geochemical and isotope data relevant to the understanding of the plumbing system, *J. Volcanol. Geotherm.*
550 *Res.*, 131, [https://doi.org/10.1016/S0377-0273\(03\)00364-1](https://doi.org/10.1016/S0377-0273(03)00364-1), 2004.

551 Francalanci, L., Davies, G. R., Lustenhouwer, W., Tommasini, S., Mason, P. R. D., and Conticelli, S.: Intra-Grain Sr Isotope
552 Evidence for Crystal Recycling and Multiple Magma Reservoirs in the Recent Activity of Stromboli Volcano, Southern Italy,
553 *J. Petrol.*, 46, <https://doi.org/10.1093/petrology/egi062>, 2005.

554 Genco, R., and Ripepe, M.: Inflation-deflation cycles revealed by tilt and seismic records at Stromboli volcano, *Geophys. Res.*
555 *Lett.*, 37, <https://doi.org/10.1029/2009GL042925>, 2010.

556 Giordano, G., and De Astis, G.: The summer 2019 basaltic Vulcanian eruptions (paroxysms) of Stromboli, *Bull. Volcanol.*,
557 83, <https://doi.org/10.1007/s00445-020-01403-0>, 2020.

558 Giudicepietro, F., Calvari, S., De Cesare, W., Di Lieto, B., Di Traglia, F., Esposito, A. M., Orazi, M., Romano, P., Tramelli,
559 A., Nolesini, T., Casagli, N., Calabria, P., and Macedonio, G.: Seismic and thermal precursors of crater collapses and overflows
560 at Stromboli volcano, *Sci. Rep.*, 13, <https://doi.org/doi.org/10.1038/s41598-023-38205-740-1038/s41598-023-30498-9>, 2023.

ha formattato: Inglese (Regno Unito)

ha formattato: Colore carattere: Rosso

Giudicepietro, F., López, C., Macedonio, G., Alparone, S., Bianco, F., Calvari, S., ... and Tramelli, A.: Geophysical precursors of the July–August 2019 paroxysmal eruptive phase and their implications for Stromboli volcano (Italy) monitoring, *Sci. Rep.*, 10, 10296, <https://doi.org/10.1038/s41598-020-67220-140.1038/s41598-020-67160-w>, 2020.

Gheri, D., Zuccarello, L., De Angelis, S., Ricci, T., and Civico, R.: Infrasonic Data from the July 4–11, 2024 Paroxysm of Stromboli Volcano [Data set]. Zenodo. <https://doi.org/10.5281/zenodo.14245572>, 2024.

Gurioli, L., Harris, A. J. L., Colò, L., Bernard, J., Favalli, M., Ripepe, M., and Andronico, D.: Classification, landing distribution, and associated flight parameters for a bomb field emplaced during a single major explosion at Stromboli, Italy, *Geology*, 41, <https://doi.org/10.1130/G33576.1>, 2013.

Harris, A., and Ripepe, M.: Temperature and dynamics of degassing at Stromboli, *J. Geophys. Res.: Solid Earth*, 112(B3), <https://doi.org/10.1029/2006JB004393>, 2007.

INGV Bulletin of 25/06/2024: <https://www.ct.ingv.it/index.php/monitoraggio-e-sorveglianza/prodotti-del-monitoraggio/bollettini-settimanali-multidisciplinari/914-bollettino-Settimanale-sul-monitoraggio-vulcanico-geochimico-e-sismico-del-vulcano-Stromboli-del-2024-06-25/file>, last access: 19 August 2024.

INGV Bulletin of 02/07/2024: <https://www.ct.ingv.it/index.php/monitoraggio-e-sorveglianza/prodotti-del-monitoraggio/bollettini-settimanali-multidisciplinari/915-bollettino-Settimanale-sul-monitoraggio-vulcanico-geochimico-e-sismico-del-vulcano-Stromboli-del-2024-07-02/file>, last access: 19 August 2024.

INGV Bulletin of 09/07/2024: <https://www.ct.ingv.it/index.php/monitoraggio-e-sorveglianza/prodotti-del-monitoraggio/bollettini-settimanali-multidisciplinari/918-bollettino-Settimanale-sul-monitoraggio-vulcanico-geochimico-e-sismico-del-vulcano-Stromboli-del-2024-07-09/file>, last access: 19 August 2024.

INGV Bulletin of 16/07/2024: <https://www.ct.ingv.it/index.php/monitoraggio-e-sorveglianza/prodotti-del-monitoraggio/bollettini-settimanali-multidisciplinari/920-bollettino-Settimanale-sul-monitoraggio-vulcanico-geochimico-e-sismico-del-vulcano-Stromboli-del-2024-07-16/file>, last access: 19 August 2024.

James, M. R., Lane, S. J., and Chouet, B. A.: Gas slug ascent through changes in conduit diameter: Laboratory insights into a volcano-seismic source process in low-viscosity magmas, *J. Geophys. Res.: Solid Earth*, 111, <https://doi.org/10.1029/2005JB003718>, 2006.

Kim, K., and Lees, J. M.: Local Volcano Infrasonic and Source Localization Investigated by 3D Simulation, *Seismol. Res. Lett.*, 85, <https://doi.org/10.1785/0220130135>, 2014.

Legrand, D., and Pertot, M.: What are VLP signals at Stromboli volcano? *J. Volcanol. Geotherm. Res.*, 421, <https://doi.org/10.1016/j.jvolgeores.2021.107429>, 2022.

Longo, R., Lacanna, G., Innocenti, L., and Ripepe, M.: Artificial Intelligence and Machine Learning Tools for Improving Early Warning Systems of Volcanic Eruptions: The Case of Stromboli, *IEEE Trans. Pattern Anal. Mach. Intell.*, 46(12), 7973–7982, <https://doi.org/10.1109/TPAMI.2024.3399689>, 2024.

Marchetti, E., and Ripepe, M.: Stability of the seismic source during effusive and explosive activity at Stromboli Volcano, *Geophys. Res. Lett.*, 32, <https://doi.org/10.1029/2005GL023962>, 2005.

ha formattato: Colore carattere: Rosso

Marchetti, E., Genco, R., and Ripepe, M.: Ground deformation and seismicity related to the propagation and drainage of the dyke feeding system during the 2007 effusive eruption at Stromboli volcano (Italy), *J. Volcanol. Geotherm. Res.*, 182, <https://doi.org/10.1016/j.jvolgeores.2009.01.029>, 2009.

McKee, K. F., Roman, D. C., Waite, G. P., and Fee, D.: Silent very long period seismic events (VLPs) at Stromboli Volcano, Italy, *Geophys. Res. Lett.*, 49(23), e2022GL100735, <https://doi.org/10.1029/2022GL100735>, 2022.

McNutt, S. R., and Nishimura, T.: Volcanic tremor during eruptions: Temporal characteristics, scaling and constraints on conduit size and processes, *J. Volcanol. Geotherm. Res.*, 178, <https://doi.org/10.1016/j.jvolgeores.2008.07.023>, 2008.

Pino, N. A., Moretti, R., Allard, P., and Boschi, E.: Seismic precursors of a basaltic paroxysmal explosion track deep gas accumulation and slug upraise, *J. Geophys. Res.: Solid Earth*, 116, <https://doi.org/10.1029/2011JB008547>, 2011.

Pistolesi, M., Delle Donne, D., Pioli, L., Rosi, M., and Ripepe, M.: The 15 March 2007 explosive crisis at Stromboli volcano, Italy: Assessing physical parameters through a multidisciplinary approach, *J. Geophys. Res.*, 116, <https://doi.org/10.1029/2011JB008527>, 2011.

Ripepe, M.: Evidence for gas influence on volcanic seismic signals recorded at Stromboli, *J. Volcanol. Geotherm. Res.*, 70, [https://doi.org/10.1016/0377-0273\(96\)00033-8](https://doi.org/10.1016/0377-0273(96)00033-8), 1996a.

Ripepe, M., Poggi, P., Braun, T., and Gordeev, E.: Infrasonic waves and volcanic tremor at Stromboli, *Geophys. Res. Lett.*, 23, <https://doi.org/10.1029/96GL02394>, 1996b.

Ripepe, M., and Gordeev, E.: Gas bubble dynamics model for shallow volcanic tremor at Stromboli, *J. Geophys. Res.: Solid Earth*, 104, <https://doi.org/10.1029/1998JB900046>, 1999.

Ripepe, M., Delle Donne, D., Lacanna, G., Marchetti, E., and Ulivieri, G.: The onset of the 2007 Stromboli effusive eruption recorded by an integrated geophysical network, *J. Volcanol. Geotherm. Res.*, 182(3-4), 131–136, <https://doi.org/10.1016/j.jvolgeores.2009.02.011>, 2009.

Ripepe, M., Delle Donne, D., Genco, R., Maggio, G., Pistolesi, M., Marchetti, E., Lacanna, G., Ulivieri, G., and Poggi, P.: Volcano seismicity and ground deformation unveil the gravity-driven magma discharge dynamics of a volcanic eruption, *Nat. Commun.*, 6(1), 6998, <https://doi.org/10.1038/ncomms7998>, 2015.

Ripepe, M., Pistolesi, M., Coppola, D., Delle Donne, D., Genco, R., Lacanna, G., ... and Valade, S.: Forecasting effusive dynamics and decompression rates by magmatic model at open-vent volcanoes, *Sci. Rep.*, 7, <https://doi.org/10.1038/s41598-017-00748-4>, 2017.

Ripepe, M., Lacanna, G., Pistolesi, M., Silengo, M. C., Aiuppa, A., Laiolo, M., ... and Delle Donne, D.: Ground deformation reveals the scale-invariant conduit dynamics driving explosive basaltic eruptions, *Nat. Commun.*, 12, 1683, <https://doi.org/10.1038/s41467-021-21722-2>, 2021a.

Ripepe, M., Delle Donne, D., Legrand, D., Valade, S., and Lacanna, G.: Magma pressure discharge induces very long period seismicity, *Sci. Rep.*, 11, <https://doi.org/10.1038/s41598-021-86061-x>, 2021b.

Ripepe, M., and Lacanna, G.: Volcano generated tsunamis recorded in the near source, *Nat. Commun.*, 15, <https://doi.org/10.1038/s41467-024-18567-x>, 2024.

ha formattato: Colore carattere: Rosso

629 Rizzo, A. L., Federico, C., Inguaggiato, S., Sollami, A., Tantillo, M., Vita, F., ... and Grassa, F.: The 2014 effusive eruption at
 630 Stromboli volcano (Italy): Inferences from soil CO₂ flux and ³He/⁴He ratio in thermal waters, *Geophys. Res. Lett.*, 42,
 631 <https://doi.org/10.1002/2015GL064152>, 2015.
 632 Rosi, M., Bertagnini, A., Harris, A. J. L., Pioli, L., Pistolesi, M., and Ripepe, M.: A case history of paroxysmal explosion at
 633 Stromboli: Timing and dynamics of the April 5, 2003 event, *Earth Planet. Sci. Lett.*, 243,
 634 <https://doi.org/10.1016/j.epsl.2006.01.035>, 2006.
 635 Rosi, M., Pistolesi, M., Bertagnini, A., Landi, P., Pompilio, M., and Di Roberto, A.: Chapter 14 Stromboli volcano, Aeolian
 636 Islands (Italy): present eruptive activity and hazards, *Geol. Soc., London, Mem.*, 37, <https://doi.org/10.1144/M37.14>, 2013.
 637 Sparks, R. S. J.: Dynamics of magma degassing, *Geol. Soc., London, Spec. Publ.*, 213,
 638 <https://doi.org/10.1144/GSL.SP.2003.213.01.07>, 2003.
 639 Suckale, J., Keller, T., Cashman, K. V., and Persson, P.-O.: Flow-to-fracture transition in a volcanic mush plug may govern
 640 normal eruptions at Stromboli, *Geophys. Res. Lett.*, 43, <https://doi.org/10.1002/2016GL068082>, 2016.
 641 Wang, S.: Finite-difference time-domain approach to underwater acoustic scattering problems, *J. Acoust. Soc. Am.*, 99,
 642 <https://doi.org/10.1121/1.414620>, 1996.